Japanese Journal of Radiology (2019) 37:380–389
https://doi.org/10.1007/s11604-019-00825-3

ORIGINAL ARTICLE

CT features of parathyroid carcinomas: comparison with benign parathyroid lesions

Koji Takumi[1] · Yoshihiko Fukukura[1] · Hiroto Hakamada[1] · Hiroaki Nagano[1] · Yuichi Kumagae[1] · Hideo Arima[2] · Akihiro Nakajo[2] · Takashi Yoshiura[1]

Received: 8 December 2018 / Accepted: 28 February 2019 / Published online: 12 March 2019

Abstract

Purpose To describe CT features of parathyroid carcinomas (PCs) by comparison with benign parathyroid lesions (BPs).

Methods This retrospective study comprised 82 patients with 76 BPs (62 adenomas and 14 hyperplastic lesions) and 6 PCs. CT features (size, short-to-long axis ratio, shape, peritumoral infiltration, homogeneity, calcification, attenuation values on unenhanced CT, and contrast enhancement during arterial and venous phases) were compared between PCs and BPs. The diagnostic performance of CT features for diagnosing PCs was calculated for these individual parameters.

Results Short-to-long axis ratio was significantly larger in PCs (0.7 ± 0.1) than in BPs (0.5 ± 0.1, $p = 0.004$). Irregular shape (33%), the presence of peritumoral infiltration (50%), and calcification (33%) were significantly more common in PCs than BPs. The contrast enhancement value was significantly lower in PCs than BPs during arterial ($p = 0.004$) and venous phases ($p = 0.044$). The 100% sensitivity criterion for the short-to-long axis ratio (≥ 0.53), enhancement during arterial phase (≤ 56.6HU), and venous phase (≤ 59.5HU) yielded accuracies (62.1%, 71.9%, and 75.4%, respectively). Irregular shape, peritumoral infiltration, and calcification showed high specificity (98.7%) and accuracy (93.9%, 95.1%, and 93.9%, respectively).

Conclusions CT features of high short-to-long axis ratio, irregular shape, the presence of peritumoral infiltration and calcification, and low contrast enhancement may aid in distinguishing PCs from BPs.

Keywords Parathyroid cancer · Parathyroid adenoma · Imaging, diagnostic · Helical CT · Neck

Abbreviations

CT	Computed tomography
^{99m}Tc-MIBI	Technetium-99m sestamibi
^{18}F-FDG-PET/CT	Fluorine-18-fluorodeoxyglucose positron emission tomography/computed tomography
ROI	Region of interest
ICC	Intraclass correlation coefficient

Introduction

Parathyroid carcinoma is a rare endocrine malignancy that accounts for about 1–5% of cases of primary hyperparathyroidism [1, 2], with some geographic variation of 1% in Europe and the USA and about 5% in Japan. Patients with parathyroid carcinoma usually have symptomatic hyperparathyroidism with serum calcium levels of 14 mg/dL or greater and significantly elevated serum parathyroid hormone levels [1–3]. However, it is difficult to diagnose parathyroid carcinomas preoperatively due to clinical features similar to those of benign parathyroid lesions [1]. For parathyroid carcinomas, the initial complete surgical resection with microscopically negative margins is the recommended treatment and offers the best chance of cure. Successful resection is dependent on preoperative suspicion and intraoperative recognition of the parathyroid carcinomas [4]. Thus, accurate preoperative diagnosis of parathyroid carcinoma is important.

Several radiological studies have characterized parathyroid carcinomas to differentiate them from benign lesions

✉ Koji Takumi
takumi@m2.kufm.kagoshima-u.ac.jp

[1] Department of Radiology, Kagoshima University Graduate School of Medical and Dental Sciences, 8-35-1 Sakuragaoka, Kagoshima City 890-8544, Japan

[2] Department of Surgical Oncology, Digestive Surgery, Breast and Thyroid Surgery, Kagoshima University Graduate School of Medical and Dental Sciences, 8-35-1 Sakuragaoka, Kagoshima City 890-8544, Japan

[5–8]. On ultrasonography, parathyroid carcinomas showed a tendency to be larger, more inhomogeneous, and hypoechoic masses with lobulated margins in comparison with parathyroid adenomas [5, 6]. Technetium-99m sestamibi (^{99m}Tc-MIBI) dual-phase scintigraphy has been reported to be useful to differentiate benign from malignant parathyroid lesions, as well as to detect parathyroid lesions [7]. Fluorine-18-fluorodeoxyglucose positron emission tomography/computed tomography (^{18}F-FDG-PET/CT) was reported to provide additional information related to the location and extent of parathyroid carcinoma [8]. Krudy et al. [9] reported the usefulness of CT examination for detecting local recurrence and distant metastases.

CT imaging has been increasingly used for preoperative detection of parathyroid lesions. Three or more phases are performed to determine the pattern of enhancement, which is one of the primary features used to identify a parathyroid adenoma and to distinguish it from thyroid nodules or lymph nodes [10–13]. Parathyroid adenomas typically demonstrate low attenuation on non-contrast CT, intense enhancement in the arterial phase, and washout of contrast on delayed phase-enhanced CT imaging [12, 13]. Only one recent report [14] showed the contrast enhancement pattern of the parathyroid carcinomas which was a relatively low washout rate. To the best of our knowledge, however, there are no published studies with systematically evaluating the CT imaging features of parathyroid carcinomas in comparison with benign lesions. Therefore, the purpose of this study was to describe the CT imaging features of parathyroid carcinomas in comparison with benign parathyroid lesions.

Materials and methods

Patients

Institutional ethics review board approval was obtained, and informed consent was waived for this retrospective study. Our institution's endocrine surgery database was queried, and 100 consecutive patients with histologically proven parathyroid lesions during the period from November 2003 to October 2015 were identified.

A total of 18 patients who did not undergo preoperative CT examinations to evaluate parathyroid lesions were excluded. The remaining 82 patients (31 men and 51 women; mean age, 63 years; range, 18–87 years) were included in the present study. For all tumors, the final diagnoses were confirmed on histopathological evaluation of surgically resected specimens. The median interval between the preoperative CT examination and surgical resection was 31 days (range for benign lesions, 2–303 days; range for carcinomas, 3–112 days).

CT imaging technique

CT was performed on either a single- or multi-detector (16 or 64) row CT scanner (Xvigor or Aquilion; Toshiba Medical Systems, Tokyo, Japan). All scans began at the hard palate and went through to the carina. Imaging parameters for the single-detector row helical CT ($n = 8$, one carcinoma and 7 benign lesions) were as follows: tube voltage, 120 kVp; gantry rotation speed, 1 s; tube current, 160 mA; detector row configuration, 3 mm; and table increment, 3 mm/rotation. Imaging parameters of multi-detector row CT were: tube voltage, 120 kVp; gantry rotation speed, 0.5 s; maximum allowable tube current, 400 mA; detector row configuration, 16×1 mm for 16-detector row CT ($n = 22$, 2 carcinomas and 20 benign lesions) or 64×0.5 mm for 64-detector row CT ($n = 52$, 3 carcinomas and 49 benign lesions); and table increment, 15 mm/rotation for 16-detector row CT and 26.5 mm/rotation for 64-detector row CT. A 3-phase CT examination (unenhanced, arterial, and venous phases) was performed in 55 patients (3 carcinomas and 52 benign lesions), a 2-phase CT examination (unenhanced and arterial (1 carcinoma and 8 benign lesions) or venous phase (6 benign lesions)) was performed in 15 patients, and a one-phase CT examination was performed in 12 patients (unenhanced in 9 patients with 1 carcinoma and 8 benign lesions, and venous phase in 3 patients with 1 carcinoma and 2 benign lesions). Arterial and portal venous phase scans were obtained at 30 and 70 s after starting the infusion of contrast medium with single-detector row CT, while they were obtained using a 5-s and 35-s delay after the bolus-tracking program detected the threshold aortic enhancement of 150 HU with multi-detector row CT. All patients received nonionic contrast material with an iodine concentration of 300 mgI/mL (Iopamiron, Bayer Schering Pharma, Osaka, Japan; or Omnipaque, Daiichi Sankyo, Tokyo, Japan). The injection dose of contrast material was 1.6 mL/kg body weight, and injection duration was fixed at 30 s.

Qualitative imaging analysis

Two radiologists (HH and HN, with 10 and 5 years of experience in head and neck radiology, respectively) independently evaluated CT features of tumor shape (regular or irregular), the presence of peritumoral infiltration, tumor homogeneity (homogeneous or heterogeneous), and the presence of calcification within the tumor. We defined the peritumoral infiltration as the absence of peritumoral fat border and the presence of irregular shape of peritumoral organ. Tumor homogeneity was rated as negative when low-density area compared with parathyroid parenchyma

which seems cystic or necrotic changes within the lesion was found. Qualitative parameters were assessed on transverse images that had effective section widths of 3 mm. Any discrepancies between the two radiologists were resolved during a third analysis session, in which a decision was reached by consulting with the third radiologist (YK, with 14 years of experience in head and neck radiology). The three radiologists had the information of the presence of parathyroid lesions and their locations, but were blinded to the pathological diagnoses. In addition, we reviewed the medical records to identify the information of ultrasonography features (tumor margin (clear or unclear), tumor homogeneity (homogeneous or heterogeneous), and the presence of calcification within the tumor).

Quantitative imaging analysis

The tumor sizes (long and short diameters) and Hounsfield unit values of all parathyroid lesions were also measured by the two radiologists. The long diameter was defined as the maximum diameter of the lesion which was measured by using multiplanar reconstruction image. And the short diameter was defined as the longest horizontal line which was 90° orthogonal to the long axis on the same image. Short-to-long axis ratio was defined as short diameter divided by long diameter. A single as-large-as-possible circular or oval region of interest (ROI) was placed within each tumor (ROI mean size, 30.3 mm^2; range, 5–225 mm^2) on the slice with the largest lesion cross-sectional area. Care was taken not to include vessel calcification, cystic or necrotic changes, or artifacts within the ROIs. Contrast enhancement was calculated as the difference of Hounsfield unit values between the unenhanced image and each enhanced image. The tumor size and Hounsfield unit values were averages of the results of two observers.

Statistical analysis

A kappa analysis was used to determine the interobserver agreement for all qualitative analyses. The intraclass correlation coefficient (ICC) was calculated to evaluate interobserver agreement of quantitative analyses. We compared attenuation values during every phase between 3 scanners using one-way analysis of variance. The tumor size (long diameter), short-to-long axis ratio (short diameter/long diameter), attenuation values on unenhanced CT, and contrast enhancement during the arterial and venous phases were compared between the parathyroid carcinomas and benign lesions using the Mann–Whitney *U* test. Fisher's exact test was used to compare CT features (tumor shape, tumor homogeneity, and the presence of peritumoral infiltration and calcification) and ultrasonography features (tumor margin, tumor homogeneity, and the presence of calcification). Three CT features with the most significant difference between carcinomas and benign lesions were selected and analyzed by univariate and bivariate logistic regression analysis to determine an optimal logistic regression model for distinguishing parathyroid carcinomas from benign lesions. The receiver-operating characteristic (ROC) analysis was generate using the MedCalc statistical software (MedCalc Software, Mariakerke, Belgium) in order to assess the ability of short-to-long axis ratio and enhancement on arterial and venous phases to differentiate parathyroid carcinomas from benign lesions. For continuous variables that were significant, the optimal threshold criterion of 100% sensitivity for diagnosing parathyroid carcinomas was used. The sensitivity, specificity, positive predictive value, negative predictive value, and accuracy of CT features for diagnosing carcinomas were calculated for these individual parameters. Additionally, we examined whether the diagnostic accuracy for parathyroid carcinomas could be improved by combining these imaging findings. McNemar test used to compare the diagnostic accuracy between CT and ultrasonography features. All data for continuous variables are presented as mean ± SD. A p value < 0.05 was considered to indicate significance in all analyses. All statistical analyses were performed using SPSS, version 23.0 (SPSS Inc., Chicago, IL, USA).

Results

Patient characteristics

Patient characteristics are presented in Table 1. Of the 82 parathyroid lesions, 76 were benign (62 adenomas and 14 hyperplastic lesions; 26 men and 50 women; mean age, 62 years; range, 18–87 years) and 6 were carcinomas (4 men and 2 women; mean age, 64 years; range, 54–74 years). Five patients had multifocal benign lesions. In these 5 patients, only the largest lesion was included in this study. All parathyroid carcinomas were in left side. Of them, three carcinomas were in superior region and three were in inferior region. For benign lesions, 13 lesions were in right superior, 35 in right inferior, 15 in left superior, and 13 in left inferior region. Two patients had multiple endocrine neoplasia type-1 (MEN-1). The mean serum calcium levels in patients with benign lesions and parathyroid carcinomas were 11.5 mg/dL (range 6.2–15.9 mg/dL) and 13.0 mg/dL (range 10.3–16.8 mg/dL), respectively ($p = 0.094$). Three cases (50%) of parathyroid carcinomas were clinically and preoperatively flagged as potential parathyroid carcinoma, and the other 3 cases were suspected as adenoma. One patient with carcinoma had a neck palpable mass, and no patients showed the recurrent nerve palsy. Eleven patients (1 carcinoma and 10 benign lesions) showed bone pain with

or without osteoporosis, and 26 patients (2 carcinomas and 24 benign lesions) had symptoms related to hypercalcemia (general fatigue, appetite loss, and kidney or urinary tract stone). All patients with parathyroid carcinomas in this study did not have any lymph node metastases.

Ultrasonography features of parathyroid lesions

Sixty-one patients (3 carcinomas and 58 benign lesions) were identified with ultrasonography features in the medical records. Unclear margin was significantly more frequent in carcinomas (2/3, 66%) than in benign lesions (1/58, 2%; $p=0.005$). Three cases (100%) of parathyroid carcinomas were rated as heterogeneous, which were significantly different from benign lesions (12/58, 21%; $p=0.013$). Calcification was significantly more frequent in carcinomas (1/3, 33%) than in benign lesions (0/58, 0%; $p=0.049$). The performances of the ultrasonography features for diagnosing parathyroid carcinoma are shown in Table 2. Unclear margin, intralesional heterogeneity, and calcification showed high accuracy (96.7%, 80.3%, 96.7%, respectively).

CT features of parathyroid lesions

Table 3 shows the differences in attenuation value between 3 different CT scanners.

CT features of parathyroid carcinomas and benign lesions are presented in Table 4. The interobserver agreements ranged from substantial to almost perfect ($\kappa=0.79$ for tumor shape, $\kappa=0.82$ for peritumoral infiltration, $\kappa=0.87$ for tumor homogeneity, and $\kappa=1.00$ for calcification). All interobserver agreements of quantitative analyses were excellent (ICC = 0.97 for tumor size, ICC = 0.82 for short-to-long axis ratio, ICC = 0.89 for unenhanced CT

Table 1 Patients' characteristics of parathyroid lesions

	Carcinomas ($n=6$)	Benign lesions ($n=76$)	p
Age (years)	63.8 ± 7.1	62.4 ± 14.0	0.964[a]
Gender (man/women)	4: 2	25: 51	0.178[b]
Serum calcium level (mg/dL)	13.0 ± 2.3	11.5 ± 1.5	0.094[a]
Location of the parathyroid lesion			
Right/left	0:6	48:28	0.004[b]
Upper/lower	3:3	28:48	0.668[b]
Symptom			
Neck palpable mass	17% (1/6)	0% (0/76)	0.073[b]
Bone pain with or without osteoporosis	17% (1/6)	13% (10/76)	1.000[b]
General fatigue or appetite loss	17% (1/6)	18% (14/76)	1.000[b]
Kidney or urinary tract stone	33% (2/6)	13% (10/76)	0.211[b]

[a]Mann–Whitney U test

[b]Fisher's exact test

Table 2 Performance of ultrasonography features in diagnosing parathyroid carcinoma

	Sensitivity (%)	Specificity (%)	PPV (%)	NPV (%)	Accuracy (%)
Unclear margin	66.7 (2/3)	98.3 (57/58)	66.7 (2/3)	98.3 (57/58)	96.7 (59/61)
Intratumoral heterogeneity	100 (3/3)	79.3 (46/58)	20.0 (3/15)	100 (46/46)	80.3 (49/61)
Calcification	33.3 (1/3)	100 (58/58)	100 (1/1)	96.7 (58/60)	96.7 (59/61)

PPV positive predictive value, *NPV* negative predictive value

Table 3 Comparison of attenuation values in parathyroid lesions between different CT scanners

	Attenuation values (HU)			p
	Single-detector row $n=8$	16-detector row $n=22$	64-detector row $n=52$	
Phases				
Unenhanced	59.5 ± 5.8	45.3 ± 9.0	50.8 ± 15.7	0.055
Arterial	132.2 ± 33.5	133.3 ± 38.6	121.2 ± 38.2	0.509
Venous	127.7 ± 13.8	127.7 ± 13.8	125.3 ± 27.6	0.777

HU Hounsfield unit

Table 4 CT features of parathyroid carcinomas and benign lesions

	Carcinomas ($n=6$)	Benign lesions ($n=76$)	p
Tumor size (mm)	22.2 ± 10.7	19.2 ± 8.1	0.423[a]
Short-to-long axis ratio (short/long diameter)	0.7 ± 0.1	0.5 ± 0.1	0.004[a]
Irregular shape	33% (2/6)	1% (1/76)	0.013[b]
Peritumoral infiltration	50% (3/6)	3% (2/76)	0.002[b]
Homogeneity	50% (3/6)	64% (49/76)	0.664[b]
Calcification	33% (2/6)	1% (1/76)	0.013[b]
Unenhanced CT value (HU)	55.2 ± 8.7	49.7 ± 14.2	0.339[a]
Contrast enhancement (HU)			
Arterial phase	27.4 ± 22.7	78.0 ± 33.9	0.004[a]
Venous phase	47.4 ± 10.5	76.2 ± 25.4	0.044[a]

[a]Mann–Whitney U test

[b]Fisher's exact test

Table 5 Logistic regression analysis of CT features for distinguishing parathyroid carcinomas from benign lesions

	Odds ratio (95% CI)	p
Univariate analysis		
Short-to-long axis ratio	78,778.5 (18.92–327,997,146.70)	0.008
Peritumoral infiltration	37.0 (4.40–311.11)	0.001
Arterial phase enhancement	0.93 (0.88–0.99)	0.019
Bivariate analysis		
Short-to-long axis ratio	45,995.24 (7.05–29,744,767,394.44)	0.021
Peritumoral infiltration	37.0 (4.40–311.11)	0.006
Short-to-long axis ratio	6136.77 (0.071–529,640,068.91)	0.133
Arterial phase enhancement	0.94 (0.88–0.99)	0.037
Peritumoral infiltration	14.91 (0.51–436.42)	0.117
Arterial phase enhancement	0.92 (0.86–0.99)	0.030

values, ICC = 0.96 for the contrast enhancement value in the arterial phase, and ICC = 0.92 for the contrast enhancement value in the venous phase).

The tumor size of parathyroid carcinomas (22.2 ± 10.7 mm) was not significantly different from that of benign lesions (19.2 ± 8.1 mm, $p = 0.423$). The short-to-long axis ratio was significantly larger in carcinomas (0.7 ± 0.1) than in benign lesions (0.5 ± 0.1, $p = 0.004$). Irregular shape was significantly more frequent in carcinomas (2/6, 33%) than in benign lesions (1/76, 1%; $p = 0.013$). Peritumoral infiltration was significantly more frequent in carcinomas (3/6, 50%) than in benign lesions (2/76, 3%; $p = 0.002$). Overall, 3 cases (50%) of parathyroid carcinomas were rated as homogeneous, which were not significantly different from benign lesions (49/76, 64%; $p = 0.664$). Calcification was significantly more frequent in carcinomas (2/6, 33%) than in benign lesions (1/76, 1%; $p = 0.013$). There was no significant difference in unenhanced CT values between carcinomas and benign lesions (55.2 ± 8.7 vs. 49.7 ± 14.2 HU, $p = 0.339$). The contrast enhancement value was significantly lower for carcinomas than for benign lesions in the arterial phase (27.4 ± 22.7 vs. 78.0 ± 33.9 HU, $p = 0.004$) and in the venous phase (47.4 ± 10.5 vs. 76.2 ± 25.4 HU, $p = 0.044$).

In univariate and bivariate logistic regression analyses, the contrast enhancement during arterial phase was significantly different between parathyroid carcinoma and benign lesions (Table 5) and was better predictor of parathyroid carcinoma compared to short-to-long axis ratio ($p = 0.037$ vs. 0.133) and peritumoral infiltration ($p = 0.030$ vs. 0.117). The area under the ROC curve of contrast enhancement on arterial phase (0.872; 95% CI 0.754–0.947) was slightly higher than that of short-to-long axis ratio (0.840; 95% CI 0.716–0.925) and contrast enhancement on venous phase (0.833; 95% CI 0.708–0.920), but did not reach statistical significance ($p = 0.868$ and 0.555, respectively).

The performances of the CT features for diagnosing parathyroid carcinoma are shown in Table 6. The 100% sensitivity criterion for the short-to-long axis ratio (≥ 0.53) yielded a specificity and accuracy of 59.2% and 62.1%, respectively. Irregular shape, peritumoral infiltration, and calcification showed high specificity (98.7%) and accuracy (93.9%, 95.1%, 93.9%, respectively). The 100% sensitivity criterion for the enhancement during arterial phase (≤ 56.6 HU) and venous phase (≤ 59.5 HU) yielded the specificities (70.7% and 74.1%, respectively) and accuracies (71.9% and 75.4%, respectively). When CT showed short-to-long axis ratio (≥ 0.53) and the enhancement during venous phase (≤ 59.5 HU), the sensitivity, specificity, and accuracy for diagnosing parathyroid carcinomas were improved (100%, 91.4% and 91.8%, respectively). No significant differences were seen in accuracy to diagnose parathyroid carcinomas between tumor margin on ultrasonography and tumor shape or peritumoral infiltration on CT ($p = 0.625$), calcification on ultrasonography and CT ($p = 1.000$).

Representative cases of parathyroid gland tumors are shown in Figs. 1, 2, and 3.

Discussion

CT findings of parathyroid carcinomas were compared with those of benign parathyroid lesions. High short-to-long axis ratio, irregular shape, the presence of peritumoral infiltration and calcification, and low contrast enhancement were significantly associated with parathyroid carcinomas. To the

Table 6 Performance of CT imaging features in diagnosing parathyroid carcinoma

	Threshold Criterion	Sensitivity (%)	Specificity (%)	PPV (%)	NPV (%)	Accuracy (%)
Short-to-long axis ratio	≥0.53	100 (6/6)	59.2 (53/76)	16.2 (6/29)	100 (53/53)	62.1 (59/82)
Irregular shape	(+)	33.3 (2/6)	98.7 (75/76)	66.7 (2/3)	94.9 (75/79)	93.9 (77/82)
Peritumoral infiltration	(+)	50.0 (3/6)	98.7(75/76)	75.0 (3/4)	96.2 (75/78)	95.1 (78/82)
Calcification	(+)	33.3 (2/6)	98.7 (75/76)	66.7 (2/3)	94.9 (75/79)	93.9 (77/82)
Enhancement						
Arterial phase	≤56.6 HU	100 (4/4)	70.0 (42/60)	18.1 (4/22)	100 (42/42)	71.9 (46/64)
Venous phase	≤59.5 HU	100 (3/3)	74.1 (43/58)	16.7 (3/18)	100 (43/43)	75.4 (46/61)
Short-to-long axis ratio (≥0.53) and venous phase enhancement (≤59.5 HU)		100 (3/3)	91.4 (53/58)	37.5 (3/8)	100 (53/53)	91.8 (56/61)

PPV positive predictive value, *NPV* negative predictive value

best of our knowledge, this is the first study to report the CT features of parathyroid carcinomas in comparison with those of benign lesions. These CT features may be useful for differentiating parathyroid carcinoma from benign lesions, and they might affect the management and therapeutic planning of patients with parathyroid lesions. Patients who were diagnosed before or during surgery and underwent en bloc resection with the adjacent structures had a local recurrence rate of 8%, and a long-term overall survival rate of 89% [4]. On the other hand, simple parathyroidectomy resulted in a local recurrence rate of 51% and a long-term survival rate of 53% [4]. Thus, accurate preoperative diagnosis of parathyroid carcinoma is important.

On physical examination, up to 70% of patients with parathyroid carcinomas present with a palpable neck mass; this is quite rare in benign disease [1]. In our study, only 17% (1/6) patients with carcinoma had a palpable neck mass and no patient had the symptom of recurrent nerve palsy. No patients with benign lesions showed those symptoms. Palpable mass or recurrent laryngeal nerve palsy in a patient with primary hyperparathyroidism may be suggestive of parathyroid carcinoma [1].

In the present results, the tumor size of parathyroid carcinomas tended to be higher than that of benign lesions, but the difference was not significant. Previous reports showed that parathyroid carcinomas were significantly larger than parathyroid adenomas [6, 15, 16]. Cheon et al. [6] reported no significant difference in tumor size between parathyroid carcinomas and benign lesions, consistent with the present result.

Previous researchers reported that morphological findings other than tumor size could indicate the presence of malignancy [5, 6]. Hara et al. [5] reported that the depth/width ratio of the lesions on ultrasonography distinguished benign from malignant parathyroid lesions. They mentioned that their result was related to the fact that parathyroid carcinomas usually have a round shape, while adenomas have an elliptical shape [5]. In the present study, the short-to-long axis ratio of parathyroid carcinomas was significantly higher than that of benign lesions, which was consistent with their results [5].

The tumor shape of parathyroid carcinomas is typically more lobulated or irregular compared with that of parathyroid adenomas [17]. The present study showed that irregular shape on CT and unclear margin on ultrasonography were significantly more associated with carcinomas than with benign lesions. Peritumoral infiltration was significantly more associated with carcinomas than with benign lesions, which was consistent with a previous ultrasonography study [6]. Thus, peritumoral infiltration may be one of the predictive features of parathyroid carcinomas. However, the present two benign lesions with peritumoral infiltration on CT were proven pathologically to be intrathyroidal parathyroid adenomas, which are parathyroid adenomas occurring ectopically within or closely adjacent to the thyroid gland. Goodman et al. [18] reported that the incidence of intrathyroidal adenomas is 1.9% in primary parathyroid lesions. It is important to be aware that it might be difficult to differentiate intrathyroidal parathyroid adenomas from carcinomas with peritumoral infiltration on CT.

The present results showed no significant difference in tumor homogeneity on CT between parathyroid benign lesions and carcinomas. Heterogeneity on ultrasonography was more commonly seen in parathyroid carcinomas, which was consistent with the previous report [5]. The reason for this discrepancy might be attributable to the difference between ultrasonography and CT. Therefore, further investigation will be needed to clarify the association between tumor homogeneity and the pathological diagnosis of parathyroid lesions. Focal calcification can be seen pathologically within parathyroid carcinomas [3, 19]. In a previous report with ultrasonography features, calcification was identified in 50% (4/8) of parathyroid carcinomas, while no benign lesion had calcification [6]. In accordance with the previous ultrasonography study, the present results showed

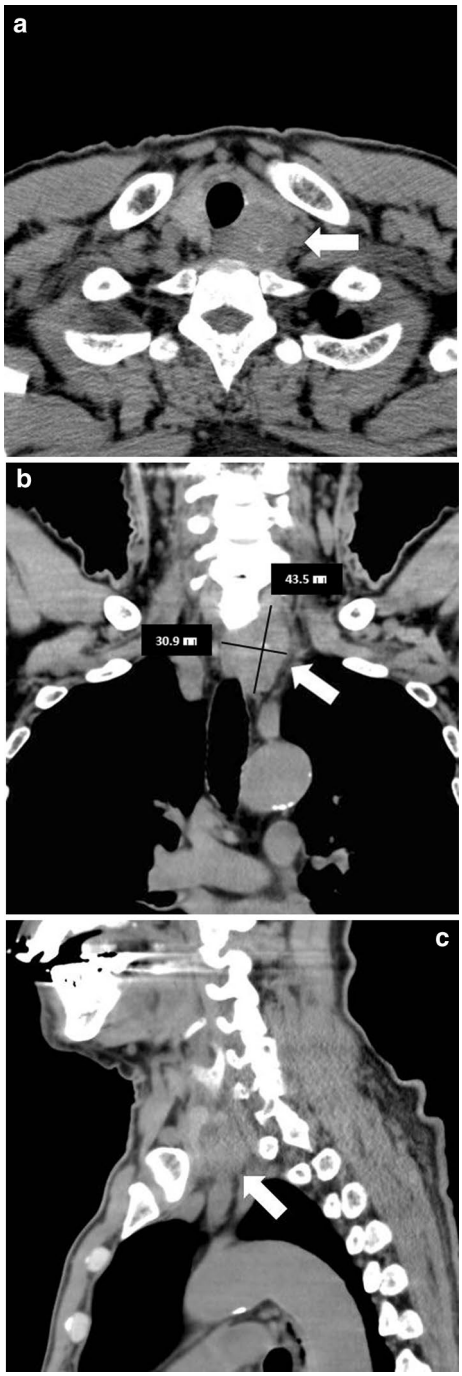

Fig. 1 A 64-year-old woman with parathyroid carcinoma. **a** Unenhanced phase CT images show a parathyroid carcinoma posterior to the inferior left thyroid lobe (arrow). **b** Para-coronal reformatted image showed 43.5 mm in long diameter and 30.9 mm in short diameter, with a short-to-long axis ratio of 0.71. The tumor has irregular shape features with intratumoral calcification

that calcification was significantly more frequent in parathyroid carcinoma than in benign lesions.

Parathyroid carcinomas showed a weak and gradual enhancement pattern. One recent study [14] showed the contrast enhancement pattern of the parathyroid carcinomas which was a relatively low washout rate (the arterial to early delayed phase, 9.29%). The reason for this discrepancy between their results and ours might be the difference of contrast enhancement protocols, the dose of contrast enhancement media, and the scan timing. Mean contrast enhancement of parathyroid carcinomas was significantly lower than that of benign lesions during the arterial phase and the venous phase, which was consistent with their results [14]. The histological characteristics of parathyroid carcinomas include angioinvasion, tumor necrosis, and fibrosis [20, 21]. Necrosis and fibrosis may be related to the weak and gradual enhancement pattern of parathyroid carcinomas. Several previous reports [22, 23] showed that lymph nodes had lower contrast enhancement in comparison with that of parathyroid adenomas, which is similar to contrast enhancement pattern of parathyroid carcinomas in this study. Therefore, it might be difficult to differentiate parathyroid carcinomas from lymph nodes only by evaluating the contrast enhancement pattern. The contrast enhancement pattern of parathyroid adenomas has been controversial. Bahl et al. [24] reported variable enhancement patterns of parathyroid adenomas by comparing with attenuation value of thyroid gland. They reported that the enhancement pattern, which was not higher in attenuation than the thyroid in the arterial phase but was lower in attenuation than the thyroid in the delayed, was most common with a prevalence of 57% of parathyroid benign lesions. Recently, Lee et al. [25] reported that large parathyroid adenomas (≥ 1 cm^3) showed early arterial enhancement and a rapid venous phase washout pattern, whereas small parathyroid adenomas (< 1 cm^3) showed a gradual enhancement pattern in the venous phase. In the present result, benign parathyroid lesions showed slight washout between the arterial and venous phases.

In the present results, a high accuracy in diagnosing carcinoma was found for the presence of irregular shape (93.9%), peritumoral infiltration (95.1%), and calcification (93.9%), which was consistent with a previous report regarding ultrasonographic features [6]. These imaging features may be useful diagnostic tools for parathyroid carcinomas. In addition, the present study showed that a 100% sensitivity criterion for the short-to-long axis ratio (≥ 0.53) and contrast enhancement during the arterial phase (≤ 56.6 HU) and the venous phase (≤ 59.5 HU) yielded accuracies of 62.1%, 71.9%, and 75.4%, respectively. Thus, a low short-to-long axis ratio (< 0.53) and high contrast enhancement (arterial phase, > 56.6 HU; venous phase, > 59.5 HU) would suggest benignity.

Clinically, scintigraphy examination, in particular ^{99m}Tc-MIBI, is widely used to detect parathyroid lesions. For differentiating malignant from benign parathyroid lesions, one previous report showed that ^{99m}Tc-MIBI dual-phase scintigraphy could differentiate parathyroid carcinomas from benign

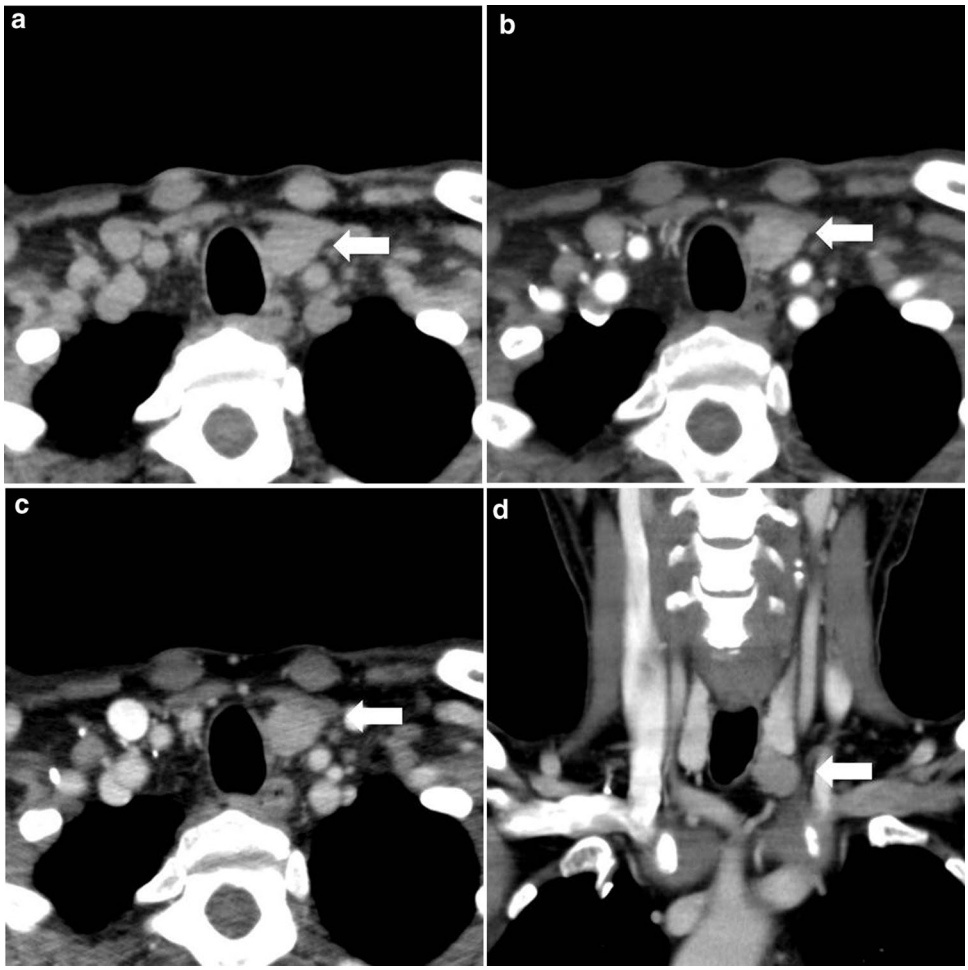

Fig. 2 A 68-year-old man with a left carotid space parathyroid carcinoma. **a** Unenhanced phase axial image shows an oval lesion measuring 19.8 mm inferior to the left thyroid lobe (arrow). **b** Arterial phase axial image shows mild enhancement in the lesion (56.6 HU) (arrow). **c** Venous phase axial image shows persistent enhancement (59.5 HU) (arrow). **d** Coronal reformatted image in the venous phase demonstrates a semi-oval lesion (arrow) with a short-to-long axis ratio of 0.77

lesions with high-intense radioactivity on delayed images (similar to or greater than submandibular gland activity) and little radioactivity difference between early and delayed images [8]. In addition, ^{18}F-FDG-PET/CT can be considered a very sensitive tool for pre- or post-surgery staging or follow-up evaluation of parathyroid carcinoma with additional information of the extension of disease, identification of recurrence, and residual disease after treatment [9]. In this study, we did not evaluate the scintigraphy features of parathyroid lesions, and however, one patient with parathyroid carcinoma underwent ^{99m}Tc-MIBI scintigraphy and showed high-intense radioactivity (similar to submandibular gland activity) on delayed phase. Two patients with carcinoma showed increased ^{18}F-FDG activity with a maximum standardized uptake value (SUV max) of 4.0 and 6.7. In this study, we evaluated the usefulness of CT features for differentiating malignant from benign lesions. CT images for parathyroid lesions are widely used and can be useful for not only detection of parathyroid lesions but evaluation of the tumor features, lesion extension, and adjacent anatomical structure in detail. We believe that it is important to diagnose and evaluate parathyroid lesions with combination of those modalities.

There are several limitations in the present study. First, because of its rarity, the number of carcinomas was small which limits the statistical power. We believe our pilot study would encourage future research, and it would be desirable to conduct a large multicenter study. Second, it was a retrospective study that may have been subject to selection bias due to an unbalanced number of patients for each type of lesion. A well-designed prospective study on CT features may be needed in the future. Third, the histopathological examination was not performed for evaluation of the characteristics which influenced the morphological features and contrast enhancement pattern. However, this is the first report to evaluate directly the difference of CT imaging features between parathyroid carcinomas and benign lesions. Further examination was needed to evaluate the radiological–pathological correlation. Finally, three different types of CT scanners were used, and this could also have affected the study results. Different imaging protocols were used in this study because of the long time frame. However, all patients underwent helical CT examinations, which allowed us to analyze all imaging criteria observed in parathyroid lesions (morphological features and attenuation).

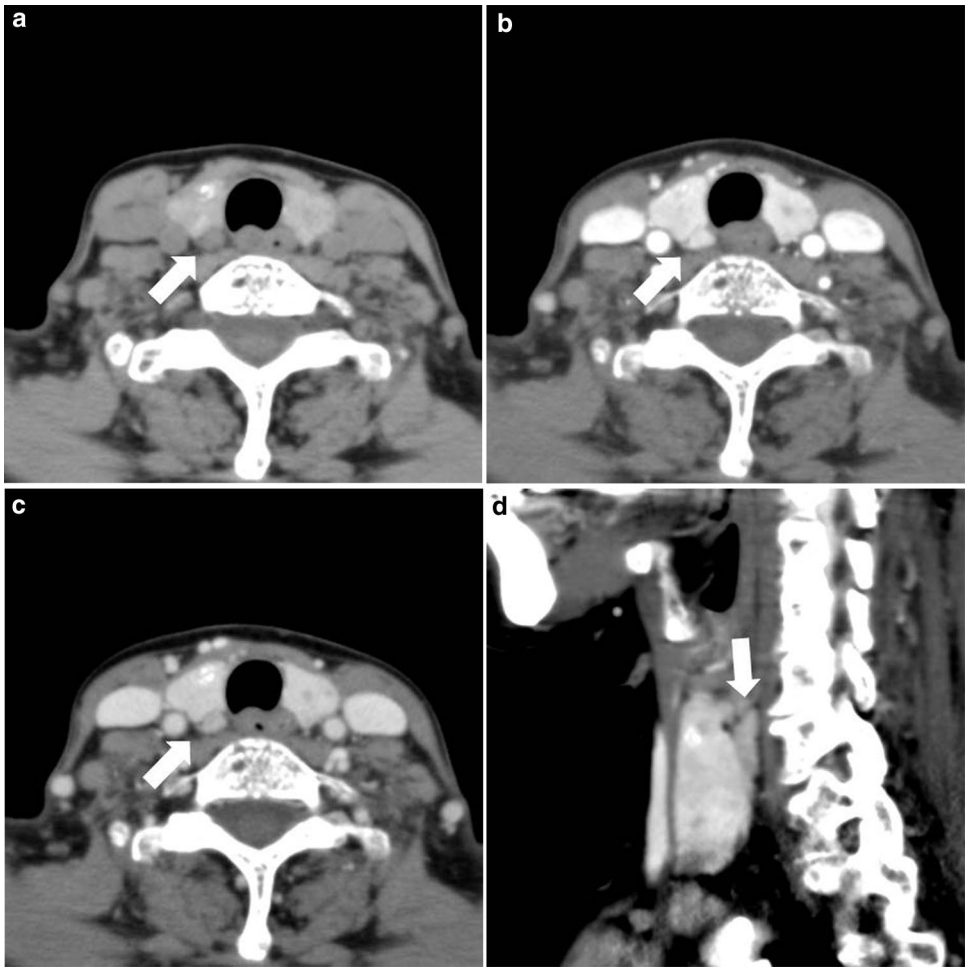

Fig. 3 A 69-year-old woman with a right parathyroid adenoma. Dynamic CT study shows a parathyroid lesion with typical enhancement characteristics and morphology. **a** Unenhanced phase axial image shows an oval lesion posterior to the right thyroid lobe (arrow). **b** Arterial phase axial image shows strong contrast enhancement (169.1 HU) (arrow). **c** Venous phase axial image shows a washout enhancement pattern (104.0 HU) (arrow). **d** Sagittal reformatted image in the venous phase shows an elliptical lesion (arrow) measuring 15.9 mm, with a short-to-long axis ratio of 0.34

In conclusion, the CT imaging characteristics of parathyroid carcinomas were described. High short-to-long axis ratio, irregular shape, the presence of peritumoral infiltration and calcification, and low contrast enhancement appear to be key CT findings to distinguish parathyroid carcinomas from benign parathyroid lesions.

Compliance with ethical standards

Conflict of interest The authors declare that they have no conflict of interest.

Ethical statement All procedures performed in studies involving human participants were in accordance with the ethical standards of the institutional and/or national research committee and with the 1964 Helsinki Declaration and its later amendments or comparable ethical standards.

Informed consent Institutional ethics review board approval was obtained, and informed consent was waived for this retrospective study.

References

1. Shane E. Clinical review 122: parathyroid carcinoma. J Clin Endocrinol Metab. 2001;86:485–93.
2. Obara T, Okamoto T, Kanbe M, Iihara M. Functioning parathyroid carcinoma: clinicopathologic features and rational treatment. Semin Surg Oncol. 1997;13:134–41.
3. Givi B, Shah JP. Parathyroid carcinoma. Clin Oncol (R Coll Radiol). 2010;22:498–507.
4. Koea JB, Shaw JH. Parathyroid cancer: biology and management. Surg Oncol. 1999;8:155–65.
5. Hara H, Igarashi A, Yano Y, Yashiro T, Ueno E, Aiyoshi Y, et al. Ultrasonographic features of parathyroid carcinoma. Endocr J. 2001;48:213–7.
6. Sidhu PS, Talat N, Patel P, Mulholl NJ, Schulte KM. Ultrasound features of malignancy in the preoperative diagnosis of parathyroid cancer: a retrospective analysis of parathyroid tumours larger than 15 mm. Eur Radiol. 2011;21:1865–73.
7. Cheon M, Choi JY, Chung JH, Lee JY, Cho SK, Yoo J, et al. Differential findings of tc-99m sestamibi dual-phase parathyroid scintigraphy between benign and malignant parathyroid lesions in patients with primary hyperparathyroidism. Nucl Med Mol Imaging. 2011;45:276–84.
8. Evangelista L, Sorgato N, Torresan F, Boschin IM, Pennelli G, Saladini G, et al. FDG-PET/CT and parathyroid carcinoma: review of literature and illustrative case series. World J Clin Oncol. 2011;2:348–54.

9. Krudy AG, Doppman JL, Marx SJ, Brennan MF, Spiegel A, Aurback GD. Radiographic findings in recurrent parathyroid carcinoma. Radiology. 1982;142:625–9.
10. Mortenson MM, Evans DB, Lee JE, Hunter GJ, Shellingerhout D, Vu T, et al. Parathyroid exploration in the reoperative neck: improved preoperative localization with 4D computed tomography. J Am Coll Surg. 2008;206:888–95.
11. Rodgers SE, Hunter GJ, Hamberg LM, Schellingerhout D, Doherty DB, Ayers GD, et al. Improved preoperative planning for directed parathyroidectomy with 4-dimensional computed tomography. Surgery. 2006;140:932–40.
12. Hoang JK, Sung WK, Bahl M, Phillips CD. How to perform parathyroid 4D CT: tips and traps for technique and interpretation. Radiology. 2014;270:15–24.
13. Gafton AR, Glastonbury CM, Eastwood JD, Hoang JK. Parathyroid lesions: characterization with dual-phase arterial and venous enhanced CT of the neck. AJNR Am J Neuroradiol. 2012;33:949–52.
14. Christakis I, Vu T, Chuang HH, Fellman B, Figueroa AMS, Williams MD, et al. The diagnostic accuracy of neck ultrasound, 4D-Computed tomographyand sestamibi imaging in parathyroid carcinoma. Eur J Radiol. 2017;95:82–8.
15. Xue S, Chen H, Lv C, Shen X, Ding J, Liu J, et al. Preoperative diagnosis and prognosis in 40 Parathyroid Carcinoma Patients. Clin Endocrinol (Oxf). 2016;85:29–36.
16. Iacobone M, Lumachi F, Favia G. Up-to-date on parathyroid carcinoma: analysis of an experience of 19 cases. J Surg Oncol. 2004;88:223–8.
17. Edmonson GR, Charboneau JW, James EM, Reading CC, Grant CS. Parathyroid carcinoma: high-frequency sonographic features. Radiology. 1986;161:65–7.
18. Goodman A, Politz D, Lopez J, Norman J. Intrathyroid parathyroid adenoma: incidence and location-the case against thyroid lobectomy. Otolaryngol Head Neck Surg. 2011;144:867–71.
19. Rawat N, Khetan N, Williams DW, Baxter JN. Parathyroid carcinoma. Br J Surg. 2005;92:1345–53.
20. Kebebew E. Parathyroid carcinoma. Curr Treat Options Oncol. 2001;2:347–54.
21. Al-Kurd A, Mekel M, Mazeh H. Parathyroid carcinoma. Surg Oncol. 2014;23:107–14.
22. Beland MD, Mayo-Smith WW, Grand DJ, Machan JT, Monchik JM. Dynamic MDCT for localization of occult parathyroid adenomas in 26 patients with primary hyperparathyroidism. AJR Am J Roentgenol. 2011;196:61–5.
23. Hunter GJ, Schellingerhout D, Vu TH, Perrier ND, Hamberg LM. Accuracy of four-dimensional CT for the localization of abnormal parathyroid glands in patients with primary hyperparathyroidism. Radiology. 2012;264:789–95.
24. Bahl M, Sepahdari AR, Sosa JA, Hoang JK. Parathyroid adenomas and hyperplasia on four-dimensional CT scans: three patterns of enhancement relative to the thyroid gland justify a three-phase protocol. Radiology. 2015;277:454–62.
25. Lee EK, Yun TJ, Kim JH, Lee KE, Kim SJ, Won JK, et al. Effect of tumor volume on the enhancement pattern of parathyroid adenoma on parathyroid four-dimensional CT. Neuroradiology. 2016;58:495–501.